Chemical trends in the structural stability of binary crystals

James R. Chelikowsky
Corporate Research Science Laboratories, Exxon Research and Engineering Company, Annandale, New Jersey 08801
(Received 8 May 1986)

The role of chemical and pressure changes on the structural stability of simple binary crystals is examined. We have considered crystals of the form $A^N B^{8-N}$ in three experimentally accessible structures: zinc blende, rocksalt, and β-Sn. The total energy of a reference crystal in these structures was calculated via a pseudopotential method as a function of charge transfer and pressure. We construct a phase diagram in pressure—charge-transfer space which enables us to predict the global behavior of this family of crystal structures. The structural boundaries of this phase diagram are in good agreement with experiment and the pressures predicted for structural transitions are in semiquantitative agreement with experiment. From our calculations we are able to define an ionicity scale based on charge transfer which predicts the critical ionicity for separating the zinc-blende and rocksalt structures. Our charge-transfer scale is consistent with the Phillips ionicity scale and provides a microscopic justification for the dielectric scale. Finally, for the case of the rocksalt structure, we can associate the band gap of this material with its structural stability relative to the zinc-blende structure. Specifically, as a function of charge transfer we find a metal-insulator transition occurs near the point when the rocksalt structure becomes stable versus a zinc-blende structure.

I. INTRODUCTION

With the advent of methods[1-12] to solve accurately the Kohn-Sham equations[13] whose solutions generate the ground-state charge density and the total energy of solids, it has become possible to describe quantitatively ground-state properties such as structure and cohesion. In this paper, we wish to use such methods to examine not the specific details of a given system, but the structural trends inherent to an entire class of materials. The goal of our study is to understand how such qualitative concepts as atomic size, or ionicity, can be related to microscopic quantities such as the crystalline charge configuration. Moreover, we wish to obtain a global picture of a class of materials in order to identify where unusual or desired properties may be found in terms of chemical composition.

The class of materials with which we initiate our studies has been examined before and is generally accepted[14-17] as a prototypical system to study the solid-state chemical bond. Namely, the binary crystal system: $A^N B^{8-N}$, where N is the number of valence electrons and (A,B) are simple metals or metalloids. This system contains no complexities associated with d electrons and has fully saturated bonding. The structures of this system can be broadly categorized as either fourfold or sixfold coordinated.[18] The fourfold-coordinated systems include the zinc-blende and wurtzite structures; the sixfold-coordinated system corresponds to the rocksalt structure. In all there are over 70 such crystals and most of them have been studied fairly extensively. Thus, a good data base exists upon which one can construct, or test, a comprehensive theory of the solid-state bond.

The approach taken here is to consider a reference crystal of this family and systematically alter its properties by altering the crystalline potential. For the changed potential, one can calculate the new structural properties of the crystal and see how they are altered. The reference crystal is chosen to be that of GaAs, a zinc-blende structure. This will allow us to start with a well-known material. We can systematically weaken the cation potential and strengthen the anion potential producing a more ionic configuration than our starting potential. For a given potential, we then calculate the ground-state properties for three structures: zinc blende, rocksalt, and β-Sn. These structures correspond to the major bonding types known for the AB family: covalent, ionic, and metallic. Moreover, for each situation we can examine the charge density and determine via a population analysis the relative ionicity of the potential and the relative stability of the structure in question. Specifically, we can determine a phase diagram for the three structures of interest as a function of the charge transferred from our reference structure (or the differences in the potential) and pressure. This figure will allow us to extract an overview of the structural stability of this crystal family as a function of pressure and ionicity or, qualitatively speaking, chemical composition.

II. COMPUTATIONAL METHODS

Of the variety of approaches that have been developed to solve the Kohn-Sham equations for total energies, the approach used here will employ pseudopotentials and linear combinations of local orbitals (Gaussians) to describe the crystalline wave functions. The method has been discussed elsewhere in some detail;[1,19] an overview is given here.

The crystalline potential can be written in the form

$$V(\mathbf{r})=\sum_{\mathbf{R},\tau} V^a(\mathbf{r}-\mathbf{R}-\tau) \quad (1)$$

and

$$V^a(\mathbf{r}) = V_i(\mathbf{r}) + V_H(\mathbf{r}) + V_{xc}(\mathbf{r}) , \quad (2)$$

where V^a is a potential centered on each atomic site, V_i is the ionic pseudopotential, V_H is the Hartree potential, and V_{xc} is the exchange-correlation potential. The ionic part of the pseudopotential is taken from the Hamann-Schluter-Chiang formalism.[20] The parameters which define the potential are given in Table I.

Initially, the Hartree potential is constructed from the wave functions obtained by solving for the isolated atom using the ionic pseudopotential V_i. Likewise, V_{xc} is constructed by using the wave functions from V_i and superposing the atomic charge in a reference crystal structure. For example, the atomic wave functions from a pseudopotential calculation for the Ga and As atoms are used in the zinc-blende structure to construct an approximate V_{xc}. The reference structure for this work is taken to be the zinc-blende structure with the known lattice constant of GaAs. We note that it is possible to construct a potential at a very different lattice constant and then check to see if the lowest energy structure is consistent with the reference structure.[1] In this case, the error in the calculated structure as compared to the reference structure is fairly small; the lattice constant changes by less than 3%. This exchange-correlation potential is then fit by a superposition of atomic site Gaussians[1,19,21] to construct V^a and the crystalline potential given by (1). This fitting procedure consisted of constructing a numerical exchange-correlation potential in real space and transforming it to reciprocal space. By assuming that the potential can be divided into a form factor and a structure factor, one can use a Gaussian expansion to fit the form factors given the known structure factor and extract the real-space form of the Gaussian expansion. A Monte Carlo simulated annealing program was used for this purpose.[21] This procedure will not properly reproduce form factors for which the structure factor vanishes, e.g., the structure factor for the $2\pi(2,2,2)/a$ reciprocal space component of the diamond lattice.[1] Moreover, it is not a unique procedure: Different expansions can yield the same potential for a given geometry, but differ as the crystal structure is altered. However, we can interpolate the form factors to estimate those for which the structure factor vanishes (in most cases they are small) and we test the transferability of our fit by comparing our results to other geometries and repeating the fitting procedure. For elemental solids, it is possible to take the atomic derived Hartree potential and the superposition of atomic charge to construct the exchange-correlation potential and use the corresponding crystalline potential to obtain accurate structural energies.[1] However, for ionic compounds, this is not the case and we include some self-consistent corrections to the total potential. Our potential for GaAs, i.e., for V^a(Ga) and V^a(As), is given in Table II. These potentials yield structural properties and a band structure for GaAs in reasonable accord with experiment.

TABLE I. Core radii r_l as defined in Ref. 20 for constructing the ionic pseudopotentials for Ga and As. The atomic configuration used for constructing the potentials was for Ga $4s^1 4p^{0.5} 3d^{0.5}$ and for As $4s^1 4p^2 3d^1$. The resulting pseudopotentials are insensitive to the details of the atomic configuration. The radii are in atomic units.

Element	r_0	r_1	r_2
Ga	1.0	1.3	2.2
As	0.9	1.1	1.6

For the ionic structures considered here, the crystalline potential can be made self-consistent in a simple, but approximate fashion. The approximate technique of Vanderbilt and Louie[19] was used for this purpose. Their technique considers the effect of interatomic charge transfer and can be outlined as follows. The self-consistent crystalline potential is written

$$V_{sc}(\mathbf{r}) = V(\mathbf{r}) + \sum_{\mathbf{R},\tau} c(\tau) g(\mathbf{r} - \mathbf{R} - \tau) , \quad (3)$$

where g is a broad Gaussian,[22] c is a coefficient of the Gaussian, and V is given by Eq. (1). The second term in (3) is to correct for charge transfer in the potentials derived from atomic properties. To construct the coefficients c, we perform a population analysis[23] and find the charge $Q(\tau)$ on site τ. One can then construct a new charge density from

$$\rho_{crys}(\mathbf{r}) = \sum_{\mathbf{R},\tau} \frac{Q(\tau)}{Q_0(\tau)} \rho_a(\mathbf{r} - \mathbf{R} - \tau) , \quad (4)$$

where $Q_0(\tau)$ is the number of valence electrons for the atom on the site τ, and ρ_a is the atomic charge density of the atom on site τ. From this crystalline density, ρ_{crys}, we can construct a new Hartree and exchange-correlation potential and determine the coefficients, c, in Eq. (3). The new potential is used to generate new $Q(\tau)$ and the population density is iterated to self-consistency. This procedure is in line with our desire to maintain an accurate description of the potential, yet not invoke the machinery for a fully self-consistent calculation. Here we have only a simple correction to the total crystalline potential; we do not have to recompute the matrix elements involving V, but only those involving a single Gaussian, g.

Once the crystalline potential has been determined, we solve the Kohn-Sham equations by using a linear combination of Gaussian orbitals. By expanding the wave functions in Gaussians and the potential, all the matrix elements can be evaluated analytically. The basis we used for the systems of interest consisted of 30 Gaussians per atom. This included two s-, three p-, and five d-like Gaussians with three different decay constants per set of orbitals. In units of a_0^{-2} (a_0 is the Bohr unit of length), the decay constants were taken to be 0.2, 0.7, and 2.0. The basis was assumed to be structurally independent in order that the calculations be tractable. Moreover, this assumption will allow us to compare charge-density populations without the arbitrariness introduced with different bases. To verify how sensitive our results are to this particular basis, we used a different basis for only eight Gaussians per atom (one s- and three p-like Gaussians with two decays of 0.2 and 0.7) and found no qualitative

TABLE II. Total crystalline pseudopotential V^a as defined in Eq. (2). The potential is expanded in Gaussians, i.e., $V^a=\sum_i a_i \exp(-b_i r^2)$. The units are in Ry for a_i and in units of a_0^{-2} (where a_0 is the bohr radius) for b_i. The pseudopotential is l dependent. For computational purposes it is easier to consider the $l=2$ potential as the local part and have $l=0,1$ corrections to this potential. Thus, differences in the $l=2$ and $l=0,1$ components are given. The potential is referenced to the known zinc-blende structure for GaAs.

V_d		V_{p-d}		V_{s-d}	
a	b	a	b	a	b
		Gallium crystalline potential			
38.576	1.047	16.267	3.696	−2.496	20.599
−89.025	0.866	−57.745	3.397	48.981	10.322
111.452	0.581	126.555	2.660	−112.231	8.030
−114.412	0.383	−236.448	1.839	179.892	5.085
80.378	0.276	324.998	1.241	−238.151	3.213
−27.375	0.215	−319.411	0.840	206.233	1.887
		225.390	0.635	−88.391	1.184
		−76.618	0.535	13.684	0.832
		Arsenic crystalline potential			
28.480	2.060	−89.160	5.066	49.611	10.979
−112.469	1.526	247.788	4.247	−147.106	8.833
199.856	1.060	−334.643	3.124	314.161	5.776
−172.057	0.739	409.316	1.988	−523.116	3.733
96.879	0.469	−336.786	1.4121	572.425	2.360
−41.514	0.361	222.126	0.874	−420.688	1.538
		−131.984	0.699	227.604	1.104
		18.520	0.522	−63.769	0.864

differences, i.e., the crystal volumes shifted in some cases by 5%; however, the relative energy differences between structures were unaffected. In evaluating the matrix elements, interactions up to the sixth, or higher, nearest neighbors were considered.

Once the eigenvalues and eigenvectors of the solid have been determined, it is possible to evaluate the total energy of the system. For this purpose, the formalism of Ihm *et al.*[24] was used. This formalism expresses the total energy in momentum space and involves the Fourier transform of the potential and charge density. The advantage of this method is that fast Fourier transform programs can be implemented. Typically, 500–1000 plane waves were incorporated in the calculation to evaluate the potential terms. To evaluate the required sums over eigenvalues, we used a ten-point–special-point **k**-point scheme[25] for the cubic structures and approximately 50 special points for the β-Sn structure. The number of these points is probably the minimum number for quantitative comparisons, i.e., an accuracy of 0.05 eV or better between structures.

An expression which incorporates the variational principle explicitly[1] was implemented for the total energy. Therefore, we have an expedited convergence of the total energy and one need not consider many iterations of the total potential. In the case of carbon in the diamond crystal structure we were able to obtain accurate total energies with effectively only one iteration.[1] For simple, binary solids we need not do more than five to six iterations in our approximate self-consistent methods and the total energy formalism outlined here.

III. GROUND-STATE PROPERTIES OF GaAs

The starting point of this study is to concentrate on the GaAs crystal. We calculate via the potentials in Table II and the method outlined above, the total energy of GaAs in the β-Sn, zinc-blende, and rocksalt structures. For each structure, we vary the lattice parameters and evaluate the total energy. One can fit an energy versus volume equation of state to our calculated energies and determine the equilibrium energy, E_0, equilibrium volume, V_0, bulk modulus, B_0, and derivative of the bulk modulus, B_0', with pressure. The equation-of-state expression is from Murnaghan:[26]

$$E(V)=B_0V[B_0'(1-V_0/V)+(V_0/V)^{B_0'}-1]\times[B_0'(B_0'-1)]^{-1}+E_0\ . \quad (5)$$

Before evaluating the total energy, we compare the energy bands for GaAs to other calculations. We display in Fig. 1 the band structure for GaAs at the known lattice constant. The calculation is in very good accord with the known valence-band spectrum;[27] the largest error we make is less than 0.25 eV. Given our local-density approximation, we do not expect the conduction bands to agree with the known optical spectrum.[28] We calculate a band gap of approximately 1.3 eV. This value is in agreement with nonrelativistic calculations for GaAs;[29] however, relativistic calculations yield a much smaller band gap.[28] In our discussion of structure, we shall be more concerned with the occupied bands and the ground-state properties. Thus, while local density makes errors in the

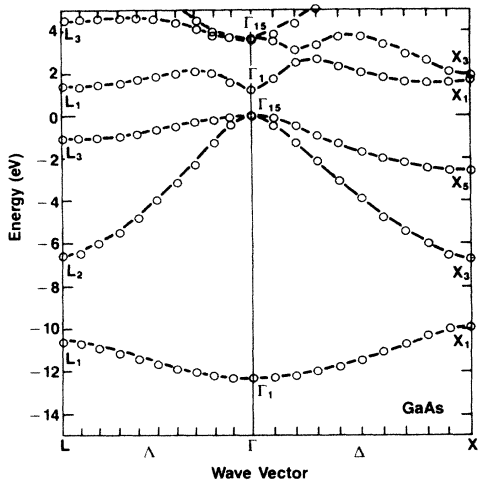

FIG. 1. Band structure of GaAs in the zinc-blende structure. The top of the valence band is referenced to zero.

optical spectrum, we can still obtain accurate values of the ground-state properties.

Once the band structure and wave functions have been evaluated, we can use Eq. (5) to extract the total energy as a function of volume. Typically, we calculate the total energy at five different volumes and fit the Murnaghan equation of state to the results. We found this equation of state to be quite accurate as judged by our fits. The largest fitting error was less than 10 meV. In Table III,[30–32] we present the calculated values for GaAs of the lattice constants, the bulk modulus, and the cohesive energy for the zinc-blende, rocksalt, and β-Sn structures. Experimental data are available for the zinc-blende structure and comparisons are made to these values. The calculated values are in satisfactory agreement with experiment, although the accuracy is not as good as fully self-consistent calculations such as the work done previously by Froyen and Cohen[33] with a plane-wave basis. In particular our lattice constant is nearly 3% too small as compared with experiment. The value Froyen and Cohen computed was too small by only 1.5%. It may be that the smaller value yielded by both calculations is characteristic of the pseudopotential approximation. For example, if we do a similar calculation for ZnSe, we find a lattice constant contracted by over 10%. We have attempted to include the Zn $3d$ electrons explicitly in our potential. In this case, we have preliminary results which suggest that if the $3d$ electrons are treated as valence electrons, the error in the lattice constant is reduced to less than 2%.

The most difficult ground-state quantity to compute is the cohesive energy. Two errors can enter the calculation. First, errors in the local density approximation may not cancel between the atom and the solid. Second, we do not solve for the atom and the solid using the same approximations. The cohesive energy we calculate is the energy difference per atom of the GaAs unit in the solid and the isolated Ga and As atoms. The theoretical value includes spin-polarized corrections for the atom;[34] the corrections were 0.18 eV for Ga and 1.54 eV for As. The total energy per each atom is -57.71 eV for Ga and -168.82 eV for As. Our calculated cohesive energy is approximately 10%

TABLE III. Ground-state properties for GaAs as calculated in the zinc-blende, rocksalt, and β-Sn structures. Experimental data are listed for the zinc-blende structure; the data are from Refs. 30–32. For the β-Sn structure, two parameters (a,c) need be specified to define the structure. The calculated values were determined by minimizing the total energy.

Structure	Cohesive energy (eV)	Lattice parameters (Å)	Bulk modulus (Mbar)
Zinc blende			
Experiment	3.6	5.65	0.75
Theory	4.1	5.48	0.86
Rocksalt	3.7	5.22	1.00
β-Sn	3.6	4.98[a] 2.81[b]	0.85

[a]For parameter a.
[b]For parameter c.

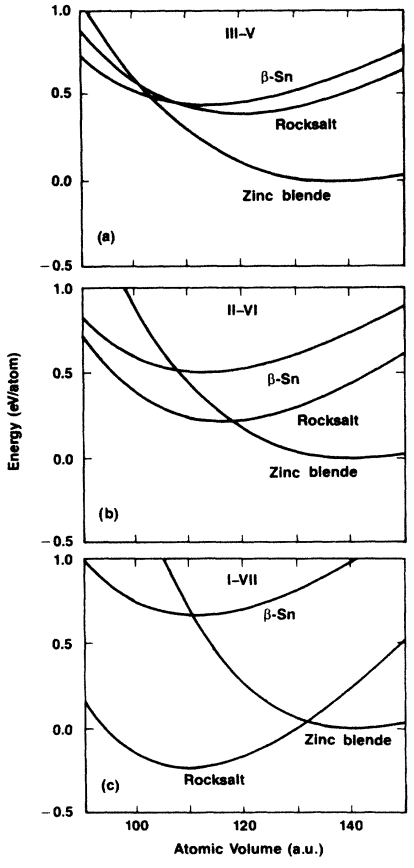

FIG. 2. (a) Equation-of-state curves for GaAs in the β-Sn, rocksalt, and zinc-blende structures. (b) Equation of state for a prototypical II-VI compound. (c) Equation-of-state curves for a prototypical I-VI compound. The energy minimum of the zinc-blende structure is taken as a reference zero.

too large; this error seems to be characteristic of the local density approximation.

In Fig. 2(a), the equation of state for GaAs is presented in the three prototypical structures. Froyen and Cohen[33] have computed similar curves for GaAs. Overall, we are in substantial agreement. However, we would predict that GaAs under pressure would transform to a β-Sn structure as opposed to the rocksalt structure. In point of fact, GaAs does neither; the structure is at present not well characterized.[35] This is consistent with our theoretical calculation in that we find the differences between rocksalt and β-Sn to be small enough to prohibit distinguishing their pressure dependences. It may be that several structures are nearly equal in free energy under pressure.[33] It is interesting that we compute a pressure transition consistent with experiment. Our calculated pressure for GaAs to transform out of the zinc-blende structure is approximately 180 kbar. The experimental values range between 160—190 kbar.[35]

IV. IONICITY TRENDS IN STRUCTURAL STABILITY

Given the computational tools to examine structural energies, we may systematically alter the GaAs crystalline potential and examine the structural stability of the three crystal types with changing ionicity. One could envision a variety of approaches to this problem. Here we construct a very simple model as a first attempt. To weaken the cation potential we have used a single Gaussian repulsive well with a fixed width roughly the size of the ion core; for the anion potential we used an identical well, but with opposite sign. This approach has the advantage of allowing us to consider a single parameter to alter the potentials: the depth of the well. The disadvantage of this approach is that changes in the well sizes may not reflect the changes in size of the cation and anion wells, i.e., orbital size effects.

One can characterize the changes in the GaAs potential by specifying the well depth of the modifying potential. However, we wish to use an index which is more readily interpretable. Thus, we examined the change in the population analysis with the changed potentials. A very strong linear correlation is found between the well depth and the charge transfer as determined from the population analysis (at very large values of the well depth the charge transfer starts to saturate). This correlation is presented in Fig. 3. We shall reference all the structural trends in terms of the charge transfer from cation to anion in terms of the figure. The reference structure here is taken to be the zinc-blende structure at the equilibrium volume in Table II. Thus, we find GaAs to have a population of approximately 2.89 a.u. on the cation and 5.11 a.u. on the anion, corresponding to a charge transfer of 0.11 electrons with respect to the isolated atoms.

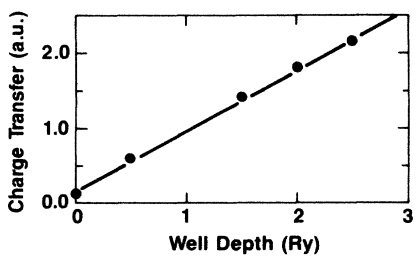

FIG. 3. Charge transfer determined by a Mulliken (Ref. 23) population analysis as function of the well depth of our model potential change (see text).

In Fig. 2, we have plotted the equation of state for three prototypical charge configurations corresponding to groups III-V, II-VI, and I-VII type semiconductors. The III-V corresponds to GaAs; the II-VI and I-VII compounds are defined by the population analysis such that the cation has II and I electrons; the anion has VI and VII electrons, respectively. Within our model it is not feasible to determine the isolated configuration in an absolute sense as we would have to separate the constituents. Unfortunately, the local-density method is flawed in that sense. If one separates GaAs to isolated atoms, one obtains $Ga^{+0.15}$ and $As^{-0.15}$ instead of the neutral species.

The qualitative result illustrated in Fig. 2 is that with an increasingly ionic configuration, the β-Sn structure moves up in energy and the rocksalt structure moves down in energy relative to the zinc-blende structure. At some configuration corresponding to a fairly ionic II-VI material, the rocksalt structure becomes more stable than the zinc-blende structure. Another interesting trend is the stability of the zinc-blende volume. This volume is hardly altered from the III-V to the II-VI configuration. If one examines the isoelectric, isocoric series Ge-GaAs-ZnSe-CuBr, this conservation of lattice constants is observed. However, this is not the case for the other ionic or metallic structures; the behavior is characteristic of a covalent structure.

One defect of our computation is evident in Fig. 2. Namely, we note that the calculated bulk moduli of all the materials increase with the charge transfer. This is probably an artifact of the fact that orbital size effects are not included when the reference crystal's potential is altered; however, we do expect the relative changes to be accurate. Again, we are attempting to examining global trends and do not expect to achieve detailed correlations with all ground-state properties. We do expect to quantify the relative structural energies quite accurately.

Given that we can determine ground-state properties as a function of charge transfer, we can define a *global* picture of crystal structure stability. A simple expression for the free energy derived from (5) is

$$G(p)=B_0V_0[(1+pB_0'/B_0)^{\gamma}-1]+E_0\ , \tag{6}$$

where $\gamma=(B_0'-1)/B_0'$, and p is pressure. By considering a sequence of different charge configurations, we can determine B_0, B_0', V_0, and E_0 as a function of charge transfer. In order to obtain the ground-state properties, B_0, B_0', V_0, and E_0, for an arbitrary charge transfer we expand each quantity as, for example,

$$B_0(\Delta Q)=a_0+a_1(\Delta Q)^2+a_2(\Delta Q)^4+a_3(\Delta Q)^6\ . \tag{7}$$

This expansion is taken for ΔQ relative to the IV-IV configuration. Thus, by symmetry we need only consider even powers for ΔQ. We obtain highly accurate fits using

TABLE IV. Expansions for the ground-state quantities: B_0, B_0', V_0, and E_0. The coefficients are defined as in Eq. (7). The values for $\Delta Q=0$ correspond to a tetravalent elemental semiconductor such as germanium and were obtained by extrapolation from our reference crystal of GaAs.

	a_0	a_1	a_2	a_3
		Zinc blende		
Bulk modulus	0.835	0.0286	0.0043	−0.0001
dB/dP	2.126	0.0085	0.0435	−0.0019
Volume	136.617	1.8742	−0.2165	0.0071
Energy	0.0	0.0	0.0	0.0
		Rocksalt		
Bulk modulus	0.884	0.0836	0.0013	0.0001
dB/dP	2.325	0.1981	0.0064	−0.0004
Volume	121.150	−1.0948	−0.0763	0.0047
Energy	0.423	−0.0059	−0.0102	0.0003
		β-Sn		
Bulk modulus	0.796	0.0953	−0.0092	0.0005
dB/dP	2.732	0.3121	−0.0553	0.0033
Volume	113.091	0.0714	0.0090	−0.0046
Energy	0.288	0.0848	−0.0076	0.0003

(7) for B_0, B_0', V_0, and E_0. The coefficients for this expansion are given in Table IV. For each structure, we considered six different charge configurations, and at least four different volumes. Hence, we performed over 70 independent band-structure calculations to obtain the information contained within Table IV.

Given the expansions in (7), we can determine $G(p)$ for each structure both as function of pressure and charge configuration. Figure 4 yields an overview of the binary crystal family. This picture is consistent with the experimentally known facts concerning this family of structures.[35–37] For example, it is well known that under pressure the diamond structure changes to β-Sn, while the more ionic structures such as the II-VI zinc blendes transform to the rocksalt structure. For the III-V's, the picture is not so clear cut as discussed above and elsewhere.[33] Physically, the overview extracted from Fig. 4 can be understood in a straightforward fashion. Under pressure, the electronic states in a covalent material become delocalized and the covalent bond becomes depleted. Such trends favor a more metallic structure such as β-Sn. The β-Sn structure stands as an intermediate structure between the diamond structure in Ge and the metallic face-centered-cubic structures such as Pb. The β-Sn structure is metallic with four nearest neighbors and two neighbors only slightly more removed. Thus, under pressure it is not surprising that it becomes favored over the diamond, or zinc-blende, structure. However, with increasing charge transfer, the rocksalt structure is clearly favored over the zinc-blende structure. The larger numbers of nearest neighbors and the higher packing density favor the electrostatic terms in rocksalt. At some value of charge transfer, the zinc-blende structure can no longer be sustained and even at zero pressure rocksalt exists. It is interesting to note that the rocksalt β-Sn boundary is rather sharp. The transition from a rocksalt to β-Sn structure happens over a rather limited area, and once rocksalt becomes favored over zinc blende at zero pressure, it is not possible to produce a rocksalt to β-Sn transition, at least for the regimes we have investigated.

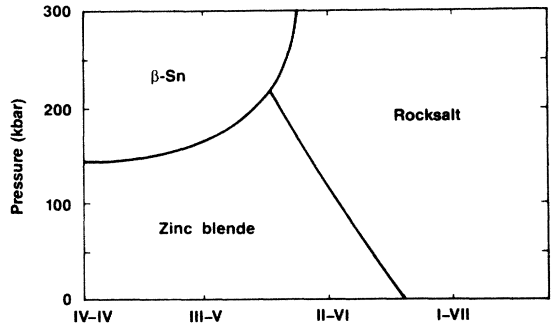

FIG. 4. Phase diagram for prototypical covalent (zinc-blende), metallic (β-Sn), and ionic (rocksalt) binary compounds. The charge configuration is referenced to the zinc-blende structure at zero pressure; however, the configuration does not change significantly from one structure to another. The diagram is based on modifying the GaAs crystalline potential and does not include orbital size effects.

One problem with Fig. 4 is that it is not clear how to place a specific binary crystal on this diagram. We need to be able to connect our charge-transfer coordinate with a known ionicity scale. Given such a connection we could place real materials on our diagram. We note that it is possible to construct an ionicity scale by employing our calculated population analyses. In analogy to the work of Coulson *et al.*,[38] we can write the ionicity of a crystal as

$$f_i(\delta Q)=(4-N)/4+\alpha\,\delta Q\ , \tag{8}$$

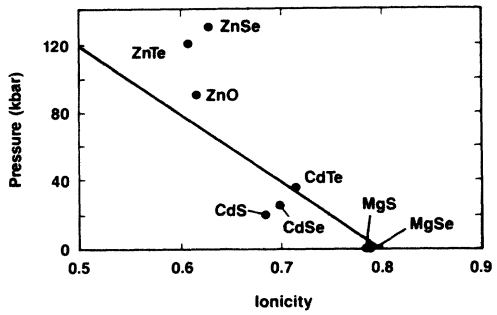

FIG. 5. Transition pressure for transformations from fourfold-coordinates II-VI compounds to sixfold-coordinated structures. The ionicity is defined from Eq. (8); the experimental data is from Refs. 14 and 37.

where N is the number of valence electrons on the cation atom, δQ is the charge transfer accompanying the formation of the solid-state system, and α is a parameter. We fix α by demanding that our value of f_i agree with the value which Phillips[14] predicts for GaAs. By doing so we can bring our scale in (8) in registry with his scale and examine the physical content of both scales. This prescription also is justified in that our calculated δQ has only relative meaning. The value which Phillips scale uses for GaAs is $f_i=0.31$. We calculate a $\delta Q=0.11$ for GaAs and exact a value of $\alpha=0.5$. We can then predict with our ionicity scale the critical ionicity, f_i^c, which divides the rocksalt and zinc-blende structures. From Fig. 4, we see that the charge configuration at the crossover point is appropriate for a II-VI material with $N=2$ and a $\delta Q=0.60$. Thus, we find $f_i^c=0.80$ in near perfect agreement with the value of the Phillips prediction of $f_i^c=0.785$. We have done a similar calculation using eight orbitals per atom and only s and p contributions to the potential and the wave functions with the resulting numbers for f_i^c being very similar. Our work suggests a microscopic basis for the quantitative existence of a critical ionicity in accord with the dielectric theory.

Moreover, by using Phillips scale we can map specific materials on to our pressure—ionicity plot. Given the uncertainties manifest in the pressure behavior of the III-V's, we indicate in Fig. 5 some II-VI materials and the pressure of transition from the zinc-blende (or wurtzite) structure to the rocksalt structure. We do not expect detailed agreement with the observed transition as our potentials as we have not considered the effects of orbital size or changes in the "covalent" bonding component. Nonetheless, we obtain semiquantitative agreement (perhaps even quantitative agreement given the large experimental uncertainties in the measured transition pressures). Specifically, we find MgSe and MgS to fall on the transition boundary from zinc blende to rocksalt at zero pressure and we are able to predict differences between Zn and Cd chalcogenides.

V. METALLICITY AND STRUCTURAL STABILITY IN ROCKSALT STRUCTURES

Given the intimate relationship between the stability of the rocksalt structure relative to the zinc-blende structure and the role of ionicity, one might ask if there exists some microscopic quantity such as the charge density which serves as a measure of the stability of the rocksalt structure. For example, a number of years ago, Walter and Cohen[39] attempted to quantify the bonding charge in semiconductors and how this bond charge was related to the stability of zinc-blende structures *vis-à-vis* rocksalt structures. They found a strong correlation between the bond charge and the critical ionicity of Phillips; however, it is now known that the bond charge need not vanish for the rocksalt structure to become stable.[33]

We wish to examine the details of this transition with respect to the band structures and optical properties for our model system as we alter the charge transfer. The result is a suggestion that the structural transition is intimately related to a metal-insulator transition, or excitonic instability, in the rocksalt structure. Consider the band structure for GaAs in the rocksalt structure [Fig. 6(a)]. This structure is metallic owing to the behavior of the X_1 conduction-band level.[40] Our band structure agrees very well with the work of Froyen and Cohen[33] for GaAs in the rocksalt structure. However, we are not interested in the details of the band structure, but rather how this band structure is altered under ionicity changes. We find the X_1 level is very sensitive to the magnitude of the antisymmetric potential, i.e., the difference in the cation and anion potentials. As the difference in the cation and anion potentials is increased, the X_1 band moves rapidly upward in energy. This change is larger than any other trend. At the structural transition we find the material has become an ideal semimetal: The gap is zero, but indirect. For larger antisymmetric potentials, an excitation gap occurs and the rocksalt structure turns into an insulator.

One can quantify the differences in the band gap and the structural stability of rocksalt versus zinc blende as a function of the charge transfer. Our starting point, the GaAs crystal, has an energy minimum in the zinc-blende structure approximately 0.4 eV below the rocksalt structure. This energy difference can be fit to a simple quadratic expression

$$\Delta E(\Delta Q)=E_{\rm rs}-E_{\rm zb}=E_0-a(\Delta Q)^2 , \tag{9}$$

where $E_0=0.4$ eV, $a=0.19$ eV/(e^2), and ΔQ is the charge in units of e transferred from the cation to anion as determined by charge populations and relative to the GaAs zinc-blende structure. Equation (9) suggests that the stabilizing force for the rocksalt structure originates in a Coulomb interaction. However, this analysis is not so transparent as one might think. Suppose one interprets ΔE as originating from a simple Madelung expression

$$\Delta E=\alpha_{\rm rs}(\Delta Q_{\rm rs})^2/R_{\rm rs}-\alpha_{\rm zb}(\Delta Q_{\rm zb})^2/R_{\rm zb} , \tag{10}$$

where $\alpha_{\rm rs},\alpha_{\rm zb}$ are Madelung sums, $\Delta Q_{\rm rs},\Delta Q_{\rm zb}$ are charge transfers, and $R_{\rm rs},R_{\rm zb}$ are nearest-neighbor distances for the rocksalt and zinc-blende crystal structures, respectively. If we take the nearest-neighbor differences from our GaAs calculation ($R_{\rm rs}=4.92$ a.u. and $R_{\rm zb}=4.48$) along with the known values for the Madelung sums ($\alpha_{\rm rs}=1.76$, $\alpha_{\rm zb}=1.64$), then we would find zinc-blende structures

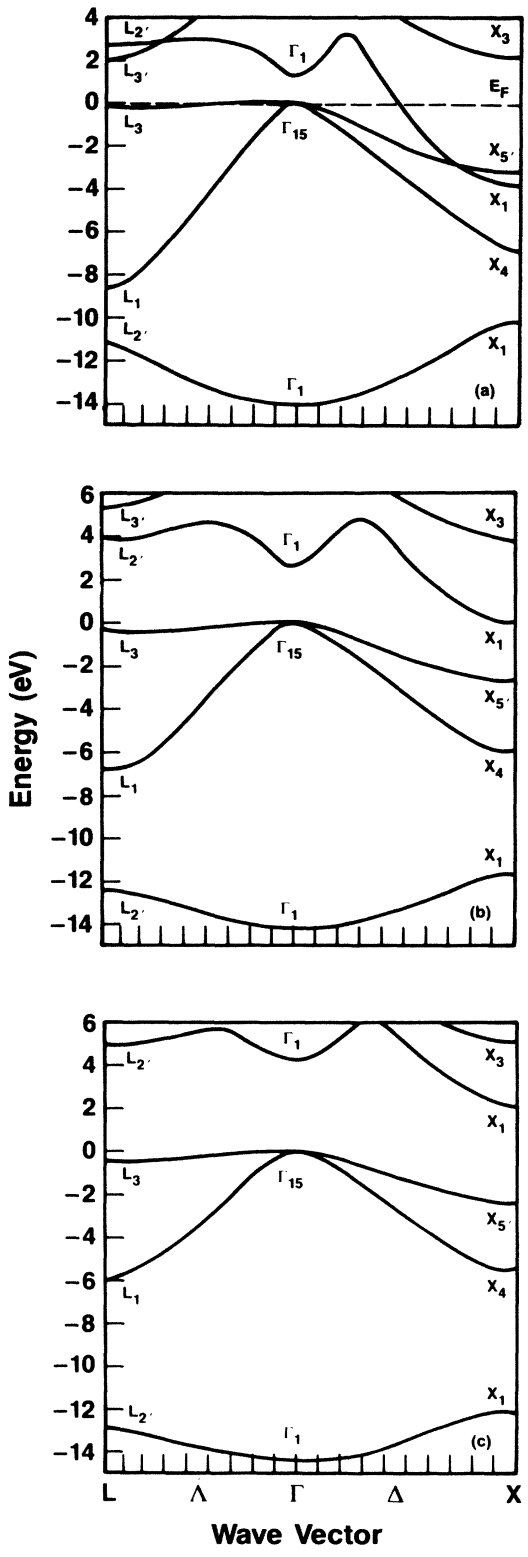

FIG. 6. Band structure of an AB crystal in the rocksalt structure. (a) Band structure of GaAs in the rocksalt structure. (b) Band structure at the critical ionicity with respect to the metal-insulator transition and with respect to the structural transition between the rocksalt and zinc-blende structures. The band gap is identically zero. (c) Band structure for a rocksalt stable compound.

favored by the Madelung sum, provided $\Delta Q_{rs}=\Delta Q_{zb}$. This somewhat surprising result is a direct consequence of the smaller nearest-neighbor distance in the zinc-blende structure. In fact, if the atomic volumes were equal, then we would find that the zinc-blende structure had a higher Madelung sum than the rocksalt structure. However, it is not true that $\Delta Q_{rs}=\Delta Q_{zb}$. In fact, we find that $\Delta Q_{rs}\sim\Delta Q_{zb}+0.1$ for a wide range of potentials. One could ascribe this larger transfer to the higher coordination number in the rocksalt structure. Another factor stabilizing the rocksalt structure via the Madelung sum is the decrease in the nearest-neighbor distance as the charge transfer increases. This is not the case for the zinc-blende structure which retains a nearly constant nearest-neighbor distance.

We also find the band gap as defined by the difference, $E_{gap}=E(\Gamma_{15})-E(X_1)$, behaves with a quadratic behavior,

$$E_{gap}=E_0^{gap}+b(\Delta Q_c)^2 . \tag{11}$$

However, we find for a similar accuracy in the fit that ΔQ_c here must be relative to the case when the anion and cation have equal charges, i.e., four electrons. We find $E_0^{gap}=-4.43$ eV and $b=0.70$ eV/(e^2). This suggests that as the compound becomes more and more covalent the metallicity of the rocksalt structure continues to be enhanced as measured by (1); however, the structural energy difference between the two crystals begins to saturate. Both the structural energy difference between the rocksalt and zinc-blende structure and the band gap as defined above as a function of the charge transfer are given in Fig. 7.

We believe the issue of a metal-insulator transition is closely coupled to the stability of the rocksalt structure; however, we are unable to offer a "proof" that the metal-insulator transition must occur in the rocksalt structure at the same charge transfer which occurs for the zinc-blende–rocksalt structural transition. Nonetheless, the band structures in Fig. 6 are highly suggestive of such a proposition. Consider the band structure of GaAs in the

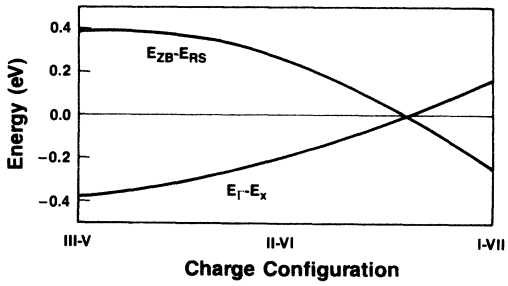

FIG. 7. Band gap of an AB rocksalt crystal and the relative structural stability of rocksalt versus zinc-blende as a function of charge transfer. The band gap in the rocksalt structure is defined here as the difference between the Γ_{15} level in the valence band and the X_1 conduction-band level. The gap has been rescaled by a factor of $\frac{1}{10}$ and is defined so that if the conduction and valence bands do not overlap the gap has a positive sign. Within computational uncertainties, the two curves cross at the same charge configuration.

rocksalt structure. The dispersion of the L_3 band is less than 0.2 eV along the Λ direction. The charge density for this state is p like and highly localized on the anion. There is some interaction with the nearest-neighbor cation along the [100] direction which accounts for the dispersion of this state along the Δ direction. However, along the [111] direction, which corresponds to the anion-anion interaction, there is virtually no interaction accounting for the extremely flat band. This band effectively pins the Fermi level at a very sharp peak in the density of states. As illustrated, the Fermi level is only 0.1 eV or less removed from Γ_{15}. The role of the anion-anion interaction in stabilizing the rocksalt structure versus the zinc-blende and cesium chloride structures has been discussed by Tosi.[41]

One might speculate that this band structure is indicative of a solid which may lower its energy by a transformation to another structure which lowers the density of states at the Fermi level. Of course, this does not necessarily imply which structure will be favored; a distorted rocksalt structure might occur. For the case of insulating GaAs in the rocksalt structure, e.g., when sufficient charge transfer occurs to raise X_1 above Γ_{15}, and a gap occurs at the Fermi level, the placement of E_f is no longer a consideration and the stability of the structure is plausible versus the zinc-blende structure.

VI. CONCLUSIONS

We have examined the $A^N B^{8-N}$ binary crystal family with respect to the stability of three prototypical structures: zinc blende, rocksalt, and β-Sn. The total energy of a reference crystal, GaAs, in these three structures was calculated with a model pseudopotential as a function of both charge transfer and pressure. Using the structural information obtained by a series of independent total energy calculations, we obtained a phase diagram for these structures in "charge-transfer–pressure" space. We found good agreement with the experimental data. For covalent compounds pressure induces a transformation from the zinc-blende to β-Sn structure; for more ionic compounds, the transformation is from the zinc-blende to rocksalt structure.

In addition, we found that at zero pressure zinc-blende transformed to rocksalt at some critical value of the ionicity. On the basis of a charge population analysis, we could define an ionicity scale. This scale is consistent with the Phillips ionicity scale in that both scales predict similar values of the ionicity for the zinc-blende to rocksalt. In addition we can use our scale to predict pressures for the zinc-blende to rocksalt transitions for II-VI semiconductors.

For the case of the rocksalt, we examined the role of metallicity on the stability of this structure versus zinc blende. We found that the band gap in the rocksalt structure correlated very strongly with the stability of this structure. Qualitatively, we expected this result; however, we found that the rocksalt structure became stable only when the band gap became positive, i.e., in terms of changing the ionicity, the structural transition occurred at the same point as the metal-insulator transition.

In summary, we note that our approach to understanding the stability of $A^N B^{8-N}$ compounds will allow us to examine global trends in a wide variety of crystal structures. We may systematically alter a number of pertinent parameters in the crystalline potential such as the well depth, well size, and angular components. As a consequence, we can ascertain structural trends and determine the origin therein from a microscopic perspective.

ACKNOWLEDGMENTS

The author would like to acknowledge helpful conversations with Professor J. K. Burdett, Professor S. G. Louie, Professor H. G. Drickamer, Professor R. Jeanloz, and Dr. H. King.

[1]J. R. Chelikowsky and S. G. Louie, Phys. Rev. B **29**, 3470 (1985).
[2]B. Harmon, W. Weber, and D. R. Hamann, Phys. Rev. B **25**, 1109 (1982).
[3]A. K. Ray and S. B. Trickey, Phys. Rev. B **24**, 1751 (1981).
[4]J. Ihm and M. L. Cohen, Phys. Rev. B **21**, 1527 (1980).
[5]M. T. Yin and M. L. Cohen, Phys. Rev. Lett. **45**, 1004 (1980).
[6]J. Callaway, X. Zou, and D. Bagayoko, Phys. Rev. B **27**, 631 (1983).
[7]F. J. Arlinghaus, J. G. Gay, and J. R. Smith, Phys. Rev. B **21**, 2055 (1980).
[8]K. M. Ho, C. L. Fu, B. N. Harmon, W. Weber, and D. R. Harmon, Phys. Rev. Lett. **49**, 673 (1982).
[9]A. K. McMahan and J. A. Moriarty, Phys. Rev. B **27**, 631 (1983).
[10]V. L. Moruzzi, J. F. Janak, and A. R. Williams, *Calculated Electronic Properties of Metals* (Pergamon, New York, 1978).
[11]G. B. Bachelet, H. S. Greenside, G. A. Baraff, and M. Schlüter, Phys. Rev. B **24**, 4745 (1981).
[12]J. W. Davenport, Phys. Rev. B **29**, 2896 (1984); J. W. Davenport, R. E. Watson, and M. Weinert, *ibid.* **32**, 4883 (1985).
[13]W. Kohn and L. Sham, Phys. Rev. **140**, A113 (1965); L. J. Sham and W. Kohn, *ibid.* **145**, 651 (1966).
[14]J. C. Phillips, Rev. Mod. Phys. **42**, 317 (1970); *Bonds and Bands in Semiconductors* (Academic, New York, 1973).
[15]A. N. Bloch and G. Schatteman, in *Structure and Bonding in Crystals,* edited by M. O'Keefe and A. Navrotsky (Academic, New York, 1981).
[16]J. K. Burdett, G. D. Price, and S. L. Price, Phys. Rev. B **24**, 2903 (1981).
[17]A. Zunger, Phys. Rev. Lett. **44**, 582 (1980).
[18]A few members of this family occur in other structures. For example, *BN* is a graphitic structure. Also, the CsCl structure includes members such as CsCl, CsBr, and CsI. For an overview of these structures, see W. B. Pearson, *The Crystal Chemistry and Physics of Metal and Alloys* (Wiley, New York, 1972).
[19]D. Vanderbilt and S. G. Louie, Phys. Rev. B **30**, 6118 (1984).
[20]D. R. Hamann, M. Schlüter, and C. Chiang, Phys. Rev. Lett. **43**, 1494 (1979).
[21]D. Vanderbilt and S. G. Louie, J. Comput. Phys. **56**, 259 (1984).
[22]Typically the Gaussian is chosen to have the form $g = \exp(-\beta r^2)$, where β is taken to be approximately d^{-2}, d

is the nearest-neighbor distance (see Ref. 19).
[23]R. S. Mulliken, J. Chem. Phys. **23**, 1833 (1955).
[24]J. Ihm, A. Zunger, and M. L. Cohen, J. Phys. C **12**, 4409 (1979).
[25]D. J. Chadi and M. L. Cohen, Phys. Rev. B **8**, 5747 (1973).
[26]F. D. Murnaghan, Proc. Natl. Acad. Sci. U.S.A. **3**, 244 (1944).
[27]J. R. Chelikowsky and M. L. Cohen, Phys. Rev. B **14**, 556 (1976).
[28]M. Hybersten and S. G. Louie, in *Proceedings of the 17th International Conference on the Physics of Semiconductors* (Springer-Verlag, New York, 1985), p. 1001; N. E. Christensen and G. B. Bachelet, *ibid.*, p. 1009. Also, D. R. Hamann, Phys. Rev. Lett. **42**, 662 (1979); S. Trickey, F. R. Green, and F. W. Averill, Phys. Rev. B **8**, 4922 (1973); J. P. Perdew and A. Zunger, *ibid.* **23**, 5048 (1981); S. Trickey, A. K. Ray, and J. P. Worth, Phys. Status Solidi B **106**, 613 (1981).
[29]U. von Barth and L. Hedin, J. Phys. C **5**, 1629 (1972).
[30]R. W. G. Wyckoff, *Crystal Structures* (Interscience, New York, 1963).
[31]As compiled by R. M. Martin, Phys. Rev. B **1**, 4005 (1970).
[32]The cohesive energy of GaAs is taken from Ref. 13.
[33]S. Froyen and M. L. Cohen, Solid State Commun. **43**, 447 (1982); Phys. Rev. B **28**, 3258 (1983); Physica **117**, 561 (1983).
[34]O. Gunnarsson, B. I. Lundqvist, and J. W. Wilkins, Phys. Rev. B **10**, 1319 (1974).
[35]A. L. Ruoff and M. A. Baublitz, Jr., *Physics of Solids Under Pressure*, edited by J. S. Schilling and R. N. Shelton (North-Holland, New York, 1981), p. 81; M. A. Baublitz, Jr. and A. L. Ruoff, J. Appl. Phys. **53**, 6179 (1982).
[36]The form of the well was taken to be $\exp(-br^2)$, with $b=0.5$ a.u.
[37]C. W. F. T. Pistorius, Prog. Solid State Chem. **11**, 1 (1976).
[38]C. A. Coulson, L. B. Redei, and D. Stocker, Proc. R. Soc. London **270**, 352 (1962). Also, see J. C. Phillips, Rev. Mod. Phys. **42**, 317 (1970).
[39]J. P. Walter and M. L. Cohen, Phys. Rev. B **4**, 1877 (1971).
[40]We use the band notation from C. Y. Fong and M. L. Cohen, Phys. Rev. Lett. **21**, 22 (1968).
[41]M. Tosi, in *Solid State Physics*, edited by H. Ehrenreich, F. Seitz, and D. Turnbull (Academic, New York, 1964), Vol. 16, p. 1.